Fluorescence anisotropy of acridinedione dyes in glycerol: Prolate model of ellipsoid

V K INDIRAPRIYADHARSHINI[a] and P RAMAMURTHY[a,b,]*

[a]National Centre for Ultrafast Processes, University of Madras, Taramani Campus, Chennai 600 113
[b]Department of Inorganic Chemistry, University of Madras, Guindy Campus, Chennai 600 025
e-mail: prm60@hotmail.com

Abstract.   Time-dependent reorientations of resorcinol-based acridinidione (ADR) dyes in glycerol were studied using steady-state and time-resolved fluorescence studies. The difference between fluorescence anisotropy decays recorded at 460 nm when exciting at 250 nm and those obtained when exciting at 394 nm are reported. When exciting at 394 nm, the fluorescence anisotropy decay is bi-exponential, while on exciting at 250 nm a mono-exponential fluorescence anisotropy decay is observed. We interpret this in terms of different directions of the absorption dipole at 394 and 250 nm with the emission dipole respectively, which is experimentally validated and further analysed as a prolate model of ellipsoid.

**Keywords.**   Fluorescence anisotropy; prolate model; acrydinedione dyes.

1. Introduction

Rotational dynamics of solutes in solvents have received much attention over the years.[1] A solute in different electronic states could have markedly different polarization decay processes in the same solvent.[2] The anisotropic rotational behaviour of small molecules has been observed with the aid of several experimental techniques[3–6] and considerable interest is shown in modelling the molecules. Reorientation times for moderate molecular sizes have been reported[7–14] using picosecond laser technique. Eisenthal and Drexhage[15] reported the first direct observation of rotational reorientation of molecules in liquid solution using picosecond laser pulses.

A fluorophore in different environments is subjected to different depolarising processes.[16] A recent study[17] of fitting in nine kinetic models also describes a system with two fluorescent species and two depolarising processes. Truong *et al*[18] have recently developed a technique used to measure the rotational dynamics of solutes in ground and excited states using optical pump/probe method. Previous findings suggest that molecules like perylene and 9-aminoacridine represent the extremes of rotational behaviour.[10,16] Barkley *et al*[16] have studied planar molecules like perylene and 9-aminoacridine in glycerol at various temperatures. The rotational dynamics of perylene are consistent with those of a disk with slip boundary conditions and that of the rotation of 9-aminoacridine are interpreted as those of prolate ellipsoid of revolution. Recently, Kunz and coworkers[19] have used fluorescence anisotropy method to probe the size of the micelle. The fluorophores used to determine the size of the micelle were acridine orange,[20] octadecylrhodamine B.[21] Kunz and coworkers[19] showed that the tetraphenyl-porphyrin dye with four di(isopropyleneglycol) methylether residues is the first fluorophore that shows single exponential decay both in fluorescence intensity and anisotropy in spherical micelle solution.

In the present study, we used resorcinol-based acridinedione (ADR) dyes with substitution as shown below. For all these dyes, the central ring adopts a boat conformation and the outer rings adopt the sofa conformation.[23]
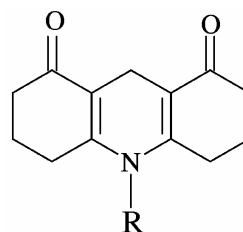
ADR	R
1	–H
2	–CH_3
3	–C_6H_5
4	–C_6H_4 (*p*-CH_3)
5	–C_6H_4 (*p*-Cl)

ADR-based dyes have been developed as a family of efficient laser dyes.[23] These dyes have structural similarity with NADH. These dyes have been shown

to mimic NADH analogues to a great extent because of their tricyclic structure, which is capable of protecting the enamine moiety.[24] These dyes function both as electron donors and acceptors and electrochemical,[25] photophysical[26] excited state reaction[27] and inclusion behaviour[28] have been investigated. The first non-conjugated bi-chromophoric system that shows dual fluorescence with an enhancement in the fluorescence intensity in the presence of transition metal ions has been studied.[29]

In the present work, we report the fluorescence anisotropy decay of ADR dyes in glycerol and its dependence on temperature at two excitation wavelengths, at which the dipole directions are different.

2. Experimental

ADR (**1–5**) dyes were synthesised by the procedure reported in the literature.[23] Glycerol used was AR grade as obtained from Qualigens, India. Absorption spectra were recorded using an Agilent 8453 diode array spectrophotometer. The excitation anisotropy spectra were recorded using a Fluoro Max 2, ISA Jobin–Yvon-Spex Instruments, S.A. Inc., USA. Fluorescence emission and emission anisotropy spectra were recorded using a Perkin–Elmer MPF-44B spectrofluorimeter interfaced with a PC through RISHCOM-100 multimeter and with the sheet polariser at the excitation and emission pathway. The fluorescence anisotropy is given by the following equation,

$$r = \frac{I_\parallel - GI_\perp}{I_\parallel + 2GI_\perp}, \tag{1}$$

where $I_\parallel$ and $I_\perp$ are the intensities observed with the emission polariser parallel or perpendicular to the polarised excitation, respectively. The G factor is the ratio of the intensity $(I_\parallel/I_\perp)$ observed with horizontally polarised excitation.[30]

Time-resolved fluorescence decays were recorded using time-correlated single-photon counting (TCSPC) technique. A diode pumped millennia V CW laser (Spectra Physics, 532 nm) was used to pump the Ti: sapphire rod in a picosecond mode-locked laser system (TSUNAMI, Spectra Physics) operated at 82 MHz. 750 and 788 nm served as the fundamental wavelengths from the Ti: sapphire laser and were passed through the pulse picker (Spectra Physics

3980 2S) to pick out 4 MHz pulses. The corresponding second (394 nm) and third (250 nm) harmonics were used for the excitation of the sample. Samples were excited through the Glan–Thompson polariser oriented in vertical and horizontal directions. The photons emitted from the sample are detected by a high gain Hamamatsu Micro Channel Plate Photomultiplier tube (R 3809U MCP-PMT). In these experiments, the fluorescence emission was collected at the magic angle (54·7°) and analysed by the reconvolution method using an iterative least squares method.[31]

The fluorescence decay $I(t)$ was analysed using an exponential function given by,

$$I(t) = B \exp(-t/\tau_f), \tag{2}$$

where B and τ_f are preexponential factors and the lifetime of the fluorophore respectively. The goodness of the fit depends upon the χ^2 (χ square) values and the distribution of the weighted residuals.

The fluorescence anisotropy decay $r(t)$ was obtained from,

$$r(t) = B_1 \exp(-t/\tau_{r1}) + B_2 \exp(-t/\tau_{r2}), \tag{3}$$

where $(B_1 + B_2) = r_0$ is the fundamental anisotropy and τ_r is the rotational correlation time. The instrument response function required in the fitting procedure was obtained by substituting the sample with the ground glass scatterer.

A sequential method for the analysis of fluorescence anisotropy decay is the direct analysis from the data. This method makes use of the decay curve $I_\parallel$ and $I_\perp$ together with the G factor, to calculate the fluorescence anisotropy decay point by point. For each set of data points a sum curve $(I_\parallel + 2GI_\perp)$ and difference curve $(I_\parallel - GI_\perp)$ is constructed and the $r(t)$ curve so obtained can then be analysed using any of the exponential fit programs in terms of number of exponential decay components; subtle errors due to convolution at the rising edge could be neglected. The G factor used in the fluorescence anisotropy measurements is measured by keeping the excitation polariser horizontal, and the polariser axes are then crossed, irrespective of the direction of the emission polariser. The relative intensities measured under these conditions were used to measure the G factor. The steady-state fluorescence and time-resolved experiments were done at various temperatures ranging from 293 to 308 K.

3. Results and discussion

3.1 *Absorption and fluorescence*

Absorption spectra of ADR (**1–5**) dyes were recorded in glycerol. These dyes show three absorption maxima around 250, 275 and 394 nm. The absorption maximum around 394 nm is assigned to the intramolecular charge transfer from the ring nitrogen to the ring carbonyl oxygen in the acridinedione fluorophore. The fluorescence spectra of ADR (**1–5**) dyes were obtained by exciting at both the wavelengths (394 and 250 nm) and the emission maximum was observed around 460 nm. Figure 1 gives the absorption and fluorescence spectrum of ADR (**4**) dye in glycerol.

3.2 *Steady state anisotropy*

The steady state excitation and emission anisotropy spectra of ADR dyes display the regions of negative and positive anisotropy. Excitation anisotropy is positive above 300 nm ($S_0 \rightarrow S_1$) and negative below 300 nm ($S_0 \rightarrow S_2$) (figure not shown). The constant emission anisotropy over the region 400–600 nm and the sharp fall in the excitation anisotropy below 300 nm is due to the involvement of higher energy electronic states. Emission anisotropy (r) data for the same dye at different temperatures is collated in table 1. The plot of r vs η/T shows linear dependency (figure 2). r values of ADR (**1–5**) dyes in glycerol are 0·29–0·33 (table 1). This positive anisotropy suggests that the emission dipoles of ADR dyes at
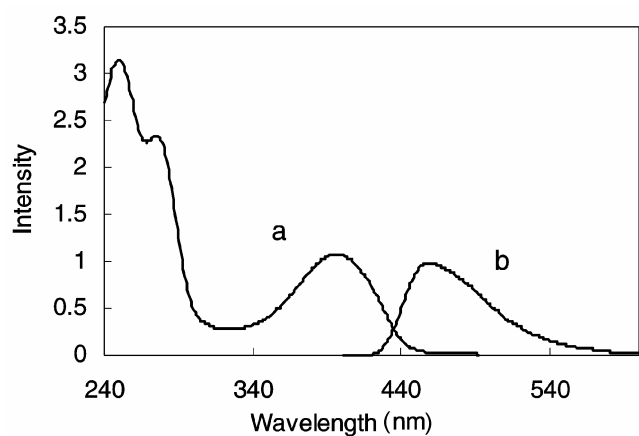
460 nm are collinear with the absorption dipole at 394 nm.

3.3 *Transition dipole directions*

Figure 3 shows the completely optimised geometry of the ADR (**3**) dye, predicted by hybrid Hartree–Fock/density functional theory method at B3LYP/6-31+G* level, using the Gaussian 03 software.[33] Calculations at B3LYP/6-31+G* level are reported to yield reliable results.[34] The molecule belongs to C_2 point group, in agreement with the sofa conformation observed from crystallographic measurements.[22] Vibrational frequency calculation confirmed that this structure is a minimum in the potential energy surface. The ADR (**3**) dye is about 0·5 Å longer along its long axis (C_5---C_{11} = 7·649 Å) than along its short axis (C_8---C_{18} = 7·147 Å). It is seen that the short axis is collinear with the C_2 symmetry axis.

The transition dipole directions of ADR (**1–5**) dyes were extracted from the Cerius 2 Zindo software. The absorption transition dipole direction at 394 nm is directed along the short axis of the molecule and at 250 nm is directed along the long axis of the molecule and is shown in figure 3 for ADR (**3**) dye.

3.4 *Fluorescence lifetime studies*

Time-dependent fluorescence measurement shows single exponential decay for ADR dyes in glycerol with lifetime varying from 5 to 8 ns (table 1). The emission decay profile of ADR (**3**) dye in glycerol recorded at 460 nm is shown in figure 4.
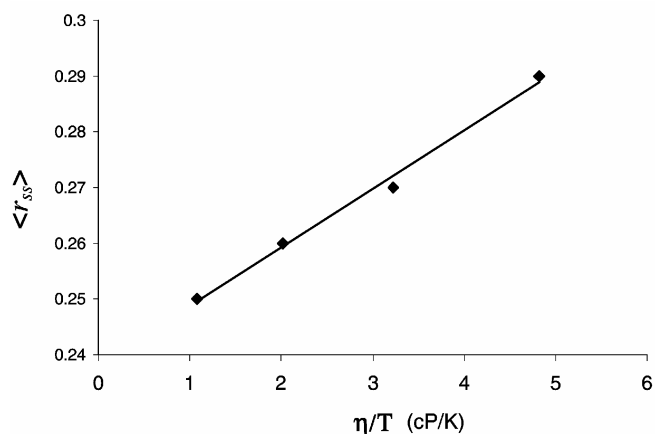

Figure 1. (a) Absorption spectrum of ADR (**4**) dye in glycerol. (b) Emission spectrum of ADR (**4**) dye in glycerol at 396 nm of excitation wavelength.

Figure 2. Plot of r vs η/T for ADR (**3**) dye in glycerol.

Table 1. Fluorescence lifetimes, emission anisotropy and decay parameters of ADR (**1–5**) dyes in glycerol at different temperatures, extracted at two excitation wavelengths.

ADR	τ_f (ns)	T (K)	$<r_{ss}>$ λ_{ex} 394 nm λ_{em} 460 nm	Single exponential λ_{ex} (250 nm) τ_r (ns)	$B1$	Bi-exponential λ_{ex} (394 nm) τ_{r1} (ns) (rel. amp)	$B1$	τ_{r2} (ns) (rel. amp)	$B2$
1	8·03	293	0·30	26·8	−0·19	1·04 (0·37)	0·03	26·8 (99·63)	0·35
		298	0·28	16·3	−0·16	0·25 (0·37)	0·08	16·2 (99·63)	0·33
		303	0·25	10·9	−0·16	0·11 (0·66)	0·05	10·9 (99·34)	0·33
		308	0·24	6·20	−0·15	0·06 (0·61)	0·08	6·19 (99·39)	0·32
2	5·00	293	0·30	11·6	−0·07	0·7 (0·10)	0·04	11·6 (99·90)	0·27
		298	0·24	10·6	−0·08	0·3 (0·16)	0·02	10·6 (99·84)	0·28
		303	0·23	7·36	−0·08	0·15 (0·09)	0·01	7·35 (99·91)	0·29
		308	0·21	4·63	−0·08	0·08 (0·03)	0·07	4·63 (99·97)	0·29
3	6·45	293	0·29	21·8	−0·13	0·49 (0·19)	0·02	21·8 (99·81)	0·25
		298	0·28	18·5	−0·13	0·48 (0·29)	0·02	18·5 (99·71)	0·25
		303	0·26	11·5	−0·11	0·25 (0·13)	0·01	11·5 (99·87)	0·23
		308	0·25	8·71	−0·12	0·17 (0·12)	0·01	8·69 (99·88)	0·23
4	8·0	293	0·33	28·7	−0·11	1·67 (0·40)	0·02	28·7 (99·60)	0·28
		298	0·31	23·7	−0·10	1·46 (0·07)	0·03	23·7 (99·30)	0·28
		303	0·29	19·7	−0·11	0·08 (0·55)	0·02	19·7 (99·45)	0·27
		308	0·27	13·6	−0·11	0·02 (0·02)	0·02	13·6 (99·98)	0·20
5	6·96	293	0·32	22·7	−0·10	0·43 (0·15)	0·02	22·7 (99·85)	0·25
		298	0·29	18·8	−0·13	0·35 (0·19)	0·02	18·8 (99·81)	0·26
		303	0·26	13·2	−0·15	0·31 (0·17)	0·01	13·3 (99·83)	0·24
		308	0·23	9·86	−0·14	0·10 (0·12)	0·01	9·84 (99·88)	0·23

Decay curves with 10000 counts at the maximum, $\chi^2 = 1\cdot1$, $<r_{ss}>$ = steady state anisotropy at excitation (394 nm) and emission (460 nm)
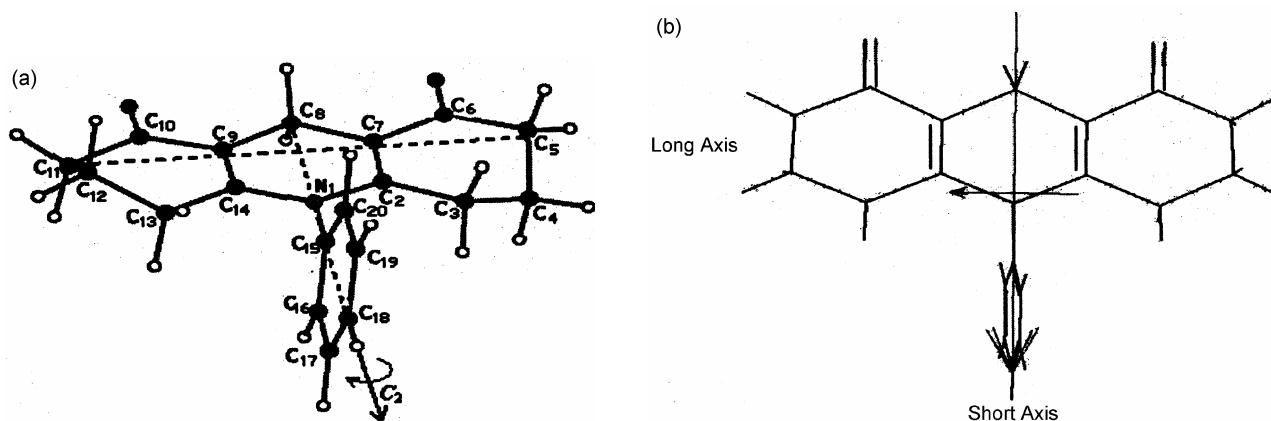

Figure 3. (**a**) B3LYP/6-31+G* optimised geometry of ADR (**3**). C_5---C_{11} = 7·649 Å (long axis); C_8---C_{18} = 7·147 Å (short axis); $C_9C_{10}C_{11}C_{12}$ = 29·5° [30·3°]; $C_{11}C_{12}C_{13}C_{14}$ = 50·3° [43·5°]; experimental values inside square brackets are for the acridinedione derivative (not shown in the figure) reported in ref. [32]. (**b**) Absorption transition dipole directions at 250 and 394 nm for ADR (**3**) dye.

3.5 *Time-resolved fluorescence anisotropy decay of ADR dyes in glycerol*

The fluorescence anisotropy decays were recorded at 460 nm with excitation at 250 and 394 nm. Fluorescence anisotropy $r(t)$ is calculated using (3) and

the decay profiles obtained on excitation at two extremes of transition moment, i.e. at 250 and 394 nm are presented in figure 5. The fluorescence anisotropy decay is biexponential on excitation at 394 nm while it is single exponential when excited at 250 nm.

The fluorescence anisotropy decay for ADR (**3**) dye in glycerol is 21·80 ns (293 K) at 250 nm and the data are shown in table 1 for other dyes. At this wavelength of excitation, the absorption and emission dipoles are near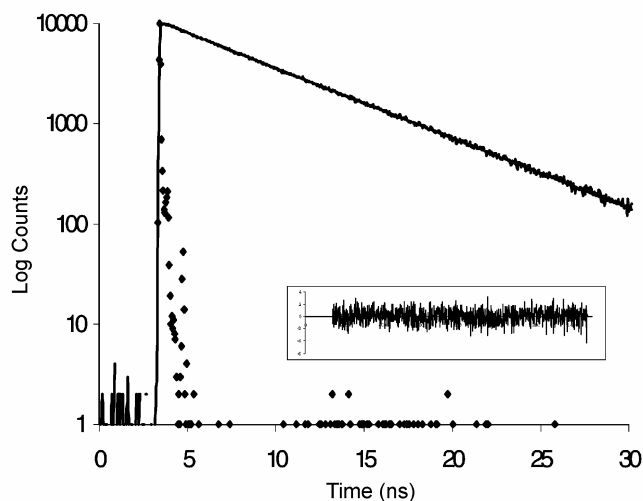ly perpendicular (scheme 1) and shows a negative fluorescence anisotropy (figure 5). Figure 5 demonstrates the decay behaviour of ADR (**3**) dye, that clearly reveals the initial fall in fluorescence anisotropy decay which then approaches zero.

Rotation along the y-axis displaces the transition moment along the z-axis, which causes depolarisation and results in one in-plane rotation. Two out-of-plane rotations along the x-axis and z-axis do not displace the transition moments. This can be compared with the fluorescence anisotropy decay of perylene, which shows fast in-plane rotation and slower out-of-plane rotation. ADR dyes show single exponential fluorescence anisotropy decay at 250 nm due to slower in-plane rotation.

The absorption and emission dipoles are nearly collinear at 394 nm (scheme 2) and show positive fluorescence anisotropy (figure 5).

The fluorescence anisotropy decay time of ADR (**3**) is 0·49 ns and 21·80 ns at 293 K (table 1). The longer fluorescence anisotropy decay time (21·80 ns) is the same as that of the fluorescence anisotropy decay time when ADR (**3**) dye is excited at 250 nm absorption band, which is assigned to the in-plane

Figure 4. Fluorescence lifetime decay of ADR (**3**) dye in glycerol at 293 K, results (residuals) for single exponential fit are shown.
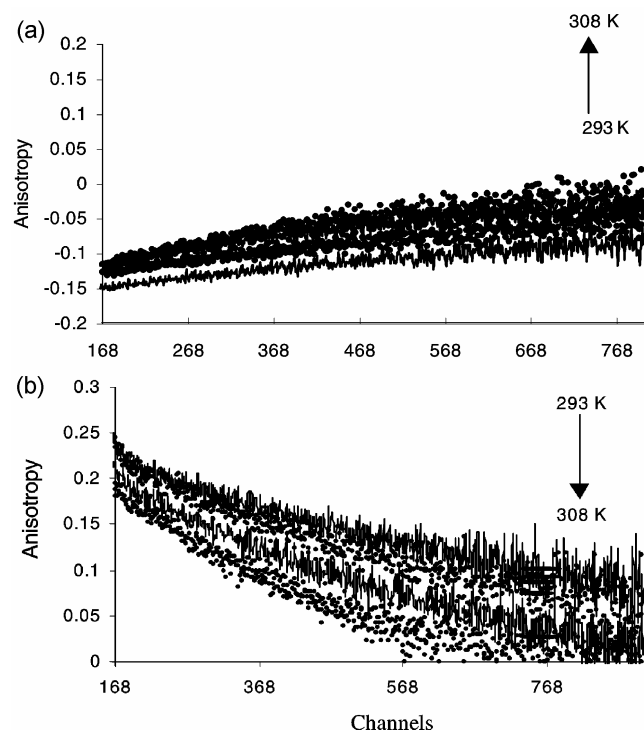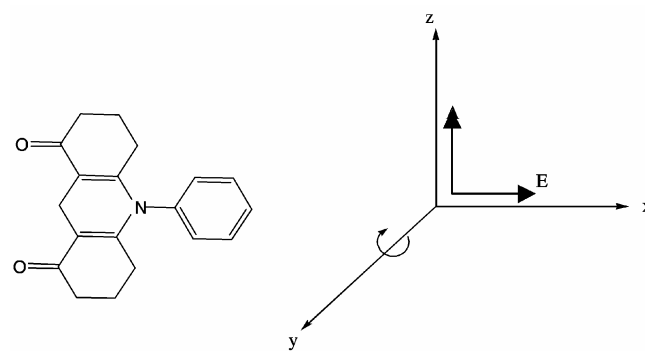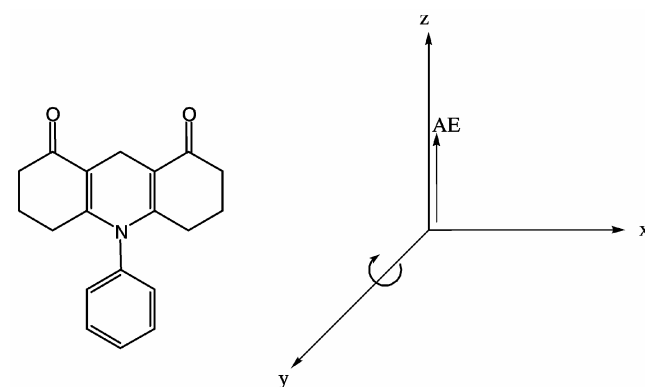

Figure 5. Fluorescence anisotropy decay of ADR (**3**) dye in glycerol from 293 to 308 K recorded at 460 nm excitation at (**a**) 250 nm (negative anisotropy) and (**b**) 394 nm (positive anisotropy).

Scheme 1.

Scheme 2.

Table 2. The angular orientation of the absorption and emission dipoles (θ_{AE}) and the diffusion coefficients of ADR (**1–5**) dyes in glycerol at different temperatures.

ADR	θ_{AE} at 250 nm	θ_{AE} at 394 nm	T (K)	$D_{\parallel} \times 10^{-9}$ (s^{-1})	$D_{\perp} \times 10^{-9}$ (s^{-1})
1	74°	20°	293	0·0062	0·2374
			298	0·0103	0·9948
			303	0·0152	2·2650
			308	0·0270	4·1540
2	63°	26°	293	0·0144	0·3503
			298	0·0157	0·8250
			303	0·0227	1·6554
			308	0·0298	3·3101
3	68°	30°	293	0·0076	0·5060
			298	0·0090	0·5163
			303	0·0145	0·9930
			308	0·0192	1·4610
4	67°	28°	293	0·0058	0·1468
			298	0·0070	0·1678
			303	0·0116	3·1190
			308	0·0122	12·490
5	70°	31°	293	0·0073	0·5780
			298	0·0089	0·7113
			303	0·0125	0·8002
			308	0·0170	2·4915

rotation. Rotation along the *y*-axis results in one in-plane rotation. Rotation along the *x*-axis and the *z*-axis results in two out-of-plane rotations, in which the *x*-axis contributes to the depolarisation. ADR dyes show biexponential fluorescence anisotropy decay due to faster out-of-plane and slower in-plane rotations. The biexponential analysis of ADR dyes in glycerol were carried out by fixing the decay time obtained at 250 nm to extract the fluorescence anisotropy decay time at 394 nm and are collated in table 1 for various temperatures. Barkley *et al*[16] interpreted the rotational dynamics of a planar molecule 9-aminoacridine, in terms of prolate ellipsoid of revolution. In 9-aminoacridine, the transition moment at 430 nm is along the long axis of the molecule and at 260 nm along the short axis of the molecule. The authors confirmed the prolate model based on the following observations: (i) the decay of the emission anisotropy is biexponential at 430 nm and monoexponential at 260 nm, and (ii) the values of $\tau_{r\,(430\,nm)}$ are less than those at $\tau_{r(260\,nm)}$. A similar observation in the present investigation suggests that the ADR dyes rotate as prolate models of ellipsoids. In the present study, we find the faster out-of-plane rotation in contrast to the earlier reports[7–14,16] for the following reasons. The calculated lengths of the long and short axes of the ADR molecule change on changing the substituent. This change in substituent

does not play any role in the faster out-of-plane rotation, instead the sofa and boat conformation of the ADR molecule makes it undergo faster out-of-plane rotation, followed by slower in-plane rotation.

The angles between the absorption and emission dipoles were calculated for ADR dyes using (4) below and are collated in table 2. The r_0 value is lower than the theoretical values that range between −0·2 and +0·4.

$$r_0 = 0.2\,(3\cos^2\theta - 1). \tag{4}$$

3.6 *Diffusion coefficients of ADR dyes in glycerol*

The theory of non-spherical molecules is usually described in terms of prolate and oblate ellipsoids. The anisotropy decay of an ellipsoid of revolution can display two or three correlation times, which are the functions of two rotational diffusion coefficients ($D_{\parallel}$ and $D_{\perp}$). The rotational correlation times are functions of rotational diffusion coefficients[35] as shown below:

$$\tau_{r1}^{-1} = 6D_{\perp}, \tag{5}$$

$$\tau_{r2}^{-1} = 2D_{\perp} + 4D_{\parallel}, \tag{6}$$

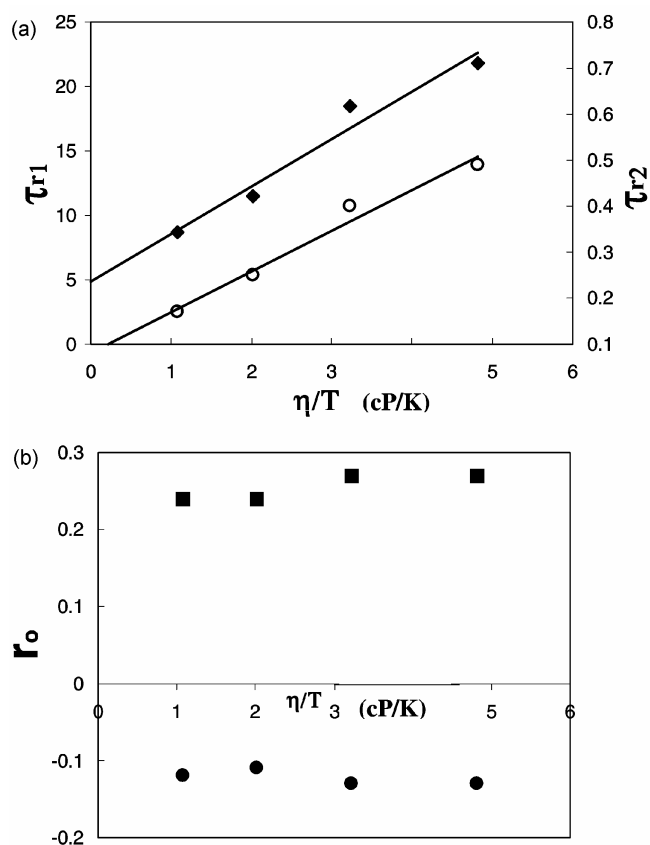$$\tau_{r3}^{-1} = 5D_{\perp} + D_{\parallel}. \tag{7}$$

Figure 6. The dependence of rotational correlation time and pre-exponential factors for ADR (**3**) dye on viscosity and temperature: (**a**) Plots of (■) τ_{r1} vs η/T and (○) τ_{r2} vs η/T; (**b**) plots of r_0 vs η/T, (■) at 394 nm (positive anisotropy) and (●) at 250 nm (negative anisotropy).

The diffusion coefficients $D_{||}$ and $D_{\perp}$ calculated from the rotational correlation times for ADR (**1–5**) dyes in glycerol are presented in table 2. The data show that the value of $D_{\perp}$ is lower than that of $D_{||}$, which is dependent on temperature. This is because the rotation about the long axis occurs with less displacement of solvent molecules when compared to rotation about the short axis.

3.7 *Temperature-dependence of ADR dyes in glycerol*

The plots of η/T vs rotational correlation time and η/T vs pre-exponential factors for the ADR (**3**) dye are shown in figure 6. Figure 6a reveals that rotational correlation time depends linearly on η/T, whereas figure 6b shows that the pre-exponential factors are independent of η/T. The strong dependence of τ_{r1} and τ_{r2} on η/T reveals the strong anisotropic rotation of ADR dyes.

4. Conclusion

In conclusion, the rotational time of ADR (**1–5**) dyes in glycerol were recorded at different temperatures using the time-resolved fluorescence technique, which are modelled as prolate ellipsoids. Interestingly, the decay of the ADR dyes exhibits the two-correlation system at short axis and the pre-exponential factors are independent of temperature and viscosity, while the rotational correlation times are dependent on temperature and viscosity. In our subsequent studies, we show how this study helps in understanding the dynamical changes in aqueous solutions of ADR molecules in β-CD nanocavity.

Acknowledgements

References

1. Fleming G R 1986 *Chemical applications of ultrafast spectroscopy* (New York: Oxford University Press); Dorfmüller Th and Pecora R (eds) 1987 *Rotational dynamics of small and macromolecules* (New York: Springer-Verlag)
2. Reiser D and Laubereau A 1982 *Opt. Commun.* **42** 329
3. Huntress W J Jr 1970 *Adv. Magn. Reson.* **4** 1
4. Goldman S A, Bruno G V, Polnaszek C F and Freed J H 1972 *J. Chem. Phys.* **56** 716
5. Vold S L, Vold R R, and Canet D 1977 *J. Chem. Phys.* **66** 1202
6. Zinsli P E 1977 *Chem. Phys.* **20** 299
7. Chuang T J and Eisenthal K B 1971 *Chem. Phys. Lett.* **11** 368
8. Phillion D W, Kuizenga D J and Siegman A E 1975 *Appl. Phys. Lett.* **27** 85
9. Fleming G R, Morris J M and Robinson G W 1976 *Chem. Phys.* **17** 91
10. Mantulin W W and Weber G 1977 *J. Chem. Phys.* **66** 4092
11. Spears K G and Cramer L E 1978 *Chem. Phys.* **30** 1
12. Von Jena A and Lessing H E 1981 *Chem. Phys. Lett.* **78** 187
13. Bauer D R, Brauman J I and Pecora R 1974 *J. Am. Chem. Soc.* **96** 6840
14. Kivelson D and Madden P A 1980 *Annu. Rev. Phys. Chem.* **31** 523
15. Eisenthal K B and Drexhage K H 1969 *J. Chem. Phys.* **51** 5720

16. Barkley M D, Kowalczyk A A and Brand L 1981 *J. Chem. Phys.* **75** 3581
17. Vyleta N P, Coley A L and Laws W R 2004 *J. Phys. Chem.* **A108** 5156
18. Truong T V and Shen Y R 2005 *J. Chem. Phys.* **122** 091104
19. Duschl J, Michl M and Kunz W 2004 *Angew. Chem. Int. Ed.* **43** 634
20. Chou S H and Wirth M J 1989 *J. Phys. Chem.* **93** 7694
21. Visser A J W G, Vos K, van Hoek A and Santema J S *J. Phys. Chem.* **92** 759
22. Sivaraman J, Subramanian K, Velmurugan D, Subramanian E and Ramakrishnan V T 1994 *Acta Crystallogr.* **C50** 2011
23. Murugan P, Shanmugasundaram P, Ramakrishnan V T, Venkatachalapathy B, Srividya N, Ramamurthy P, Gunasekaran K and Velmurugan D 1998 *J. Chem. Soc., Perkin Trans. 2* 999
24. Singh S, Chhina S, Sharma V K and Sachdev S S 1982 *J. Chem. Soc., Chem. Commun.* 453
25. Srividya N, Ramamurthy P, Shanmugasundaram P and Ramakrishnna V T 1996 *J. Org. Chem.* **61** 5083
26. Srividya N, Ramamurthy P and Ramakrishnan V T 1998 *Spectrochim. Acta* **54** 245
27. Venkatachalapathy B and Ramamurthy P 1999 *Phys. Chem. Chem. Phys.* **1** 2223
28. Indirapriyadharshini V K, Karunanithi P and Ramamurthy P 2001 *Langmuir* **17** 4056
29. Thiagarajan V, Selvaraju C, Padmamalar E J and Ramamurthy P 2004 *Chem. Phys. Chem.* **5** 1200
30. Lakowicz J R 1999 *Principle of fluorescence spectroscopy* 2nd edn (New York: Plenum)
31. O'Connor D V and Phillips D 1984 *Time correlated single photon counting* (London: Academic Press)
32. Jeyakanthan J *et al* 2002 *Crystallogr. Res. Technol.* **37** 1029
33. Frisch M J *et al* 2004 Gaussian '03, Revision B.04 Gaussian, Inc., Wallingford, CT
34. Foresman J B and Frish A 1996 *Exploring chemistry with electronic structure methods* (Pittsburgh, PA: Gaussian)
35. Tao T 1969 *Biopolymers* **8** 609